

Query Time Optimized Deep Learning Based Video Inference System

Mingren Shen[†], Shuoxuan Dong[†], and Xiuyuan He[†]

[†]Department of Computer Sciences, University of Wisconsin - Madison, 1210 W Dayton St, Madison, WI 53706

December 15, 2022

Abstract

This is a project report about how we tune Focus[1], a video inference system that provides low cost and low latency, through two phases. In this report, we will decrease the query time by saving the middle layer output of the neural network. This is a trade-off strategy that involves using more space to save time. We show how this scheme works using prototype systems, and it saves 20% of the time. The code repository URL is here, https://github.com/iphyer/CS744_FocusIngestOpt.

1 Introduction

Video inference system has received increasing attention due to its potential in various real-world applications. By querying a video data set, we can answer questions like which frames contain objects of certain classes, such as certain types of cars, pedestrians, and bicycles. Answering these questions are very useful in different areas like traffic control, video surveillance, etc [1].

Some may argue that video inference can be done using the same approach for image recognition, however, many existing image recognition methods are too expensive to be directly applied to video inference tasks. Even with state-of-the-art Convolutional Neural Networks (CNN) such as the Faster R-CNN [2] running on powerful GPUs the speed is still relatively low and computational cost is high. According to literature [1], Faster R-CNN runs 30-80 fps on a \$ 4000 GPU and it can cost up to \$ 250 to query a month-long traffic camera video on cloud. This may seem to be affordable for videos from single camera, but imagine if you have videos from thousands of cameras need to be queried, the cost is will be prohibitively high.

One of the cutting-edge video inference system that provides low cost and low latency is called Focus[1]. It uses an unique architecture that divide the video query

problem into two phases: ingesting and querying. A cheap CNN is used in the ingesting phase to quickly generate Top-K indexes which contains K possible classes of the image. An expensive CNN is then used to generate a final and more accurate prediction during query time.

For this project, we build our system based on the Focus architecture as shown in Fig 1. We propose to reuse the intermediate results of the shared layers(red trapezoid in Fig 1) between the cheap and expensive CNN to reduce inference time. Sharing convolution layers between two neural networks has already been used in Faster R-CNN model to speed up object detection where two networks, region proposal neutral network and Fast R-CNN [3], share the beginning several convolution layers [4, 2].

In this report, We show how we use two CNNs, ResNet-50 and ResNet-152, to represent the architecture of Focus [1] and we evaluate the accuracy and latency of it as our baseline. We then develop two different layer-sharing strategies. In one case the two networks share the first 4 blocks with each other, and in another case they share 7 blocks. The results suggest that depends on how many layers the two CNNs share, there is a 10% to 20% improvement for inference latency, as shown in Table 1.

2 Background

2.1 Video Inference System

Video inference system is an important area of computer vision research and application. Video inference systems often try to answer “after-the-fact” queries such as : “In all the recent 24 hours surveillance videos from 1st ave to 5th ave, return all the frames containing a truck.” Such types of questions are frequently asked by local police and other agencies [1]. NoScope and Focus are two state-of-the-art systems designed to answer these questions. This report is mainly based on Focus.

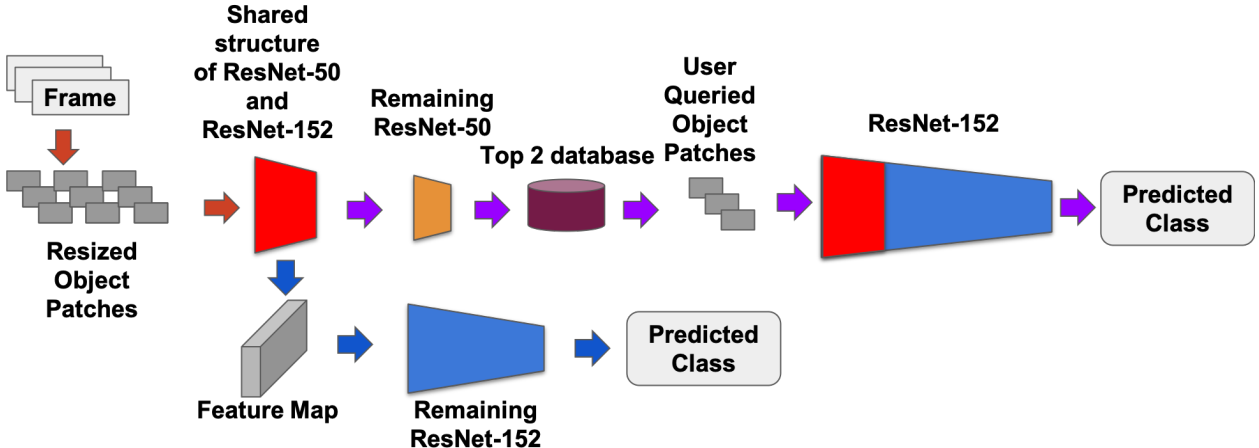


Figure 1: Project System Design

As mentioned above, Focus has two phases: ingesting and querying. During ingesting time, Focus uses a cheap CNN model, ResNet-18 [5], to pick the Top-K Indexes for each frame. For example, if the original image is a truck, the index can be a list of classes like [boat, car, truck, bus]. The first prediction on that list may not be the most accurate one. However, the top-K list almost always contain the class “truck”. During querying time, a user can query for a certain class like “truck”. With the Top-K Indexes from ingesting time, the system identifies the frames that are possibly interesting to the query. An expensive CNN model, ResNet-152, is then used to do predictions only on the selected frame set, whose index contains the specified class user queried. Such an expensive model can cost $8\times$ more compared to its cheaper variant ResNet-18, but can yield more accurate results.

2.2 Convolutional Neural Networks

Convolutional Neural Networks(CNNs) are a special class of neural network that use many layers of convolution filters to automatically extract hierarchical helpful features for the final task like classification. For example, for image classification task, beginning layers of CNNs try to learn lower-level features such as dots, lines and edges. Layers in the middle tend to build object parts based on those lower-level features and layers near the output are learning the most semantic and high-level object related information. Finally, a score is computed for each image class as output [6].

Since Krizhevsky et al. won ImageNet competition in 2012 [7], CNNs are the most popular methods for image related tasks [6]. In 2015, a new deep residual learning method called ResNet [5] even surpassed human performance on image classification tasks of Ima-

geNet. ResNet contains many stacked basic units called blocks to solve the degradation problem encountered in training deep neural network [5]. The central idea is that by attaching an identity mapping with skip connections, even very deep layers in ResNet can get the identical input from previous layer and the newly added layer should not perform worse than the shallower model [5].

CNNs are not only useful for image related tasks, they can also be used for videos [1, 8, 9] inference and tracking, recommender systems [10], natural language processing [11], and physics [12], chemistry [13, 14], material sciences [15, 16, 17, 18, 19, 20, 21, 22, 23] or medical image [24, 25, 26] and other problems [27, 28, 29, 30].

2.3 Traffic Video Characteristic

One important characteristic of surveillance or traffic camera videos is that large portion of the frames from the video is duplicate and useless, for example, if the scene is nearly static. So processing each frame is less efficient. To address this problem, NoScope [9] uses a difference detector that measures the Mean Square Error (MSE) between images to determine whether the content of the frame has changed. Compared with NoScope, Focus uses a different approach to solve the duplicate frame problem. It clusters the frames based on the output of the penultimate (i.e., previous-to-last) layer [1].

We create our data-set based on the traffic camera video frames from Urban Tracker Dataset [31]. The patches containing objects are extracted from the original images using background subtraction. The patches are labeled with 3 classes including pedestrians, cars and some subtracted background. The models are trained with manually labeled image patches.

2.4 Feature Map

Feature Maps or Feature Vectors is the intermediate output from certain CNN layers. They are abstract visual features and high-level representation of the original images. Feature maps can gradually capture higher level features that consist of lower level features. Caching feature maps in memory or save them to disk can save inference time for further uses. Xu et al. developed an effective CNN cache system to store these feature maps and reuse them at fine spatial granularity to get high performance when doing inference in continuous mobile vision [32]. Indeed, the data volume of feature maps is large, so there might be a trade off between efficiency(inference time) and storage (memory) to reuse feature maps.

3 Design

3.1 Dataset Generation

A video from the Urban Tracker Dataset [31] is used to generate object patches. To convert video into object patches, we use background subtraction to detect the moving objects (cars, pedestrians, etc.). The detector we use is BackgroundSubtractorGMG in OpenCV, which is an algorithm that combines per-pixel Bayesian segmentation with statistical background image estimation [33]. We generate 2275 patches with 3 classes: cars, pedestrians and background images (noise generated by background sub-tractor), as shown in Fig 2. All patches are re-scaled to 224x224 pixels.

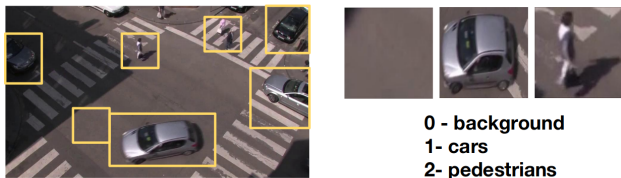


Figure 2: Background Subtraction and Generated Patches

3.2 Building Baseline

We jointly use two networks to mimic the two CNNs architecture of Focus [1]. Like Focus, we use a cheap CNN for ingest phase, during which top-k indexes are generated. During query time, the user queries frames containing a specified class. An expensive CNN is used to classify the images only if the top-k index of the image contains the desired object class.

3.3 Feature Map Reuse

Focus uses ResNet-18 and 152 as the cheap and expensive CNN, whose structure is shown in Fig 3. From that figure, we can find that the two CNNs have some same structure layers since the input layer. Considering there are two different residual blocks in ResNet [5], the basic block and the bottleneck block, we only reuse shared layers if the two models are built upon the same residual blocks. For example, if comparing ResNet-18 and ResNet-34, the two model are both built with basic blocks, and the first two residual blocks have the exact same structure. Another example would be ResNet-50 and ResNet-152, both are built with bottleneck blocks and they share the same structure for the first seven blocks. By reusing the shared structure of two networks, we try to reduce computation amount during the query phase.

3.4 Overall Experiment Design

We run our experiment based on ResNet-50 and 152, in this way we can skip more blocks, compared with ResNet-18 and 34.

During ingest time, we classify all the patches using ResNet-50 and generates Top-3 indexes. At the same time, we save the feature map for the first several residual blocks and reuse it as the input of the expensive CNN. Here we tested two cases: one is reusing the first 4 blocks and another is reusing the first 7 blocks. For the query phase, we run the expensive model to predict on the feature map. We evaluate the performance with and without retrain the remaining layers of the model.

4 Evaluation

A ResNet-50 model and a ResNet-152 are trained on the data-set we mentioned above¹. The ratio of training set and testing set is 4:1. We also retrain the remaining part of ResNet-152 with the feature maps that are output from the shared layers of the trained ResNet-50. All training curves are shown in the Appendix. The models are able to achieve almost 1 on training data-set and 0.95 to 0.97 on the testing data-set.

The developed system with trained model parameters is tested on a laptop computer to evaluate the latency of inference². The performance results of the inference system are shown in table 1. For each scenario, the test is done 5 times to show average and standard deviation of latency.

¹Our system is built on the basis of a Keras-ResNet repository on Github <https://github.com/raghakot/keras-resnet>

²Dell Inspiron 7000 laptop with a i7-6700hq CPU and 16 GBs of memory.

layer name	output size	18-layer	34-layer	50-layer	101-layer	152-layer
conv1	112×112					
conv2_x	56×56	$\left[\begin{array}{c} 3 \times 3, 64 \\ 3 \times 3, 64 \end{array} \right] \times 2$	$\left[\begin{array}{c} 3 \times 3, 64 \\ 3 \times 3, 64 \end{array} \right] \times 3$	$7 \times 7, 64, \text{stride } 2$ $3 \times 3 \text{ max pool, stride } 2$ $\left[\begin{array}{c} 1 \times 1, 64 \\ 3 \times 3, 64 \\ 1 \times 1, 256 \end{array} \right] \times 3$	$1 \times 1, 64$ $3 \times 3, 64$ $1 \times 1, 256$	$1 \times 1, 64$ $3 \times 3, 64$ $1 \times 1, 256$
conv3_x	28×28	$\left[\begin{array}{c} 3 \times 3, 128 \\ 3 \times 3, 128 \end{array} \right] \times 2$	$\left[\begin{array}{c} 3 \times 3, 128 \\ 3 \times 3, 128 \end{array} \right] \times 4$	$1 \times 1, 128$ $3 \times 3, 128$ $1 \times 1, 512$	$1 \times 1, 128$ $3 \times 3, 128$ $1 \times 1, 512$	$1 \times 1, 128$ $3 \times 3, 128$ $1 \times 1, 512$
conv4_x	14×14	$\left[\begin{array}{c} 3 \times 3, 256 \\ 3 \times 3, 256 \end{array} \right] \times 2$	$\left[\begin{array}{c} 3 \times 3, 256 \\ 3 \times 3, 256 \end{array} \right] \times 6$	$1 \times 1, 256$ $3 \times 3, 256$ $1 \times 1, 1024$	$1 \times 1, 256$ $3 \times 3, 256$ $1 \times 1, 1024$	$1 \times 1, 256$ $3 \times 3, 256$ $1 \times 1, 1024$
conv5_x	7×7	$\left[\begin{array}{c} 3 \times 3, 512 \\ 3 \times 3, 512 \end{array} \right] \times 2$	$\left[\begin{array}{c} 3 \times 3, 512 \\ 3 \times 3, 512 \end{array} \right] \times 3$	$1 \times 1, 512$ $3 \times 3, 512$ $1 \times 1, 2048$	$1 \times 1, 512$ $3 \times 3, 512$ $1 \times 1, 2048$	$1 \times 1, 512$ $3 \times 3, 512$ $1 \times 1, 2048$
	1×1			average pool, 1000-d fc, softmax		
FLOPs		1.8×10^9	3.6×10^9	3.8×10^9	7.6×10^9	11.3×10^9

Figure 3: ResNet architecture and two different cuts. The red color reuses 4 blocks and the blue one reuses 7 blocks.

It is observed that the feature map reusing models with weights trained from original structures cause huge loss in accuracy, which means that the feature maps from the shared layers of ResNet-50 model can not be fully understood by ResNet-152 although they have the same dimension. So, retrain the remaining layers of ResNet-152 would be the proper way to build the system without accuracy sacrifice.

We are able to achieve a 9.6% reduction of query time for the shallow cut retrained model with a compromise of 0.9% accuracy. Moreover, we get 17.5% reduction of query time for the deep cut retrained model with no accuracy reduction.

5.2 Other Video Inference Systems

Besides Focus, NoScope is another system for accelerating neural network query speed over videos [9]. To reduce the cost of doing Neural Network inference, NoScope uses a specialized shallower model that is less generalized but faster. The specialized model estimates the class of the objects in the frame with a confidence score. If the confidence is not high enough, a more accurate but higher cost model will be called to generate the final class for this object. However, NoScope is limited since it relies binary classifiers which is hard to scale.

6 Future work

First, our system needs to be tested on other datasets with more images and more classes. The current dataset contains just small patches of 3 different classes with a low resolution. Testing on more higher resolution datasets can prove the robustness of the system. We would also like to explore strategies of reusing layers on different ResNet models, e.g. combine ResNet-18 and 152, on the inference time. A generic methodology for deciding where to cut the layers would be useful which may need the statistics of the time consumed on each layer. Moreover, we currently only focus on ResNet architecture, which imposes restrictions for the application of this system. Other types of models should also be considered.

Since we are building our system on top of Focus [1]. The other features in Focus should be realized in our system and some of these features can even be optimized. For example, the clustering of objects in Focus can help reduce duplication of object patches, only uses simple incremental clustering method which is well-studied

Model	Accuracy	Accuracy Reduction	Latency(sec/image)	Latency Standard Deviation	Latency Reduction
ResNet-50 + 152 (Focus Baseline)	0.967	N/A	0.3611	0.0038	N/A
Reuse Feature Map (shallow cut)	0.518	46.4%	0.3277	0.0072	10.6%
Reuse Feature Map (shallow cut, retrained)	0.958	0.9%	0.3266	0.0069	9.6%
Reuse Feature Map (deep cut)	0.391	59.6%	0.3058	0.0078	15.3%
Reuse Feature Map (deep cut, retrained)	0.969	0%	0.2978	0.0070	17.5%

Table 1: System performance of difference cuts

in [1, 37, 38]. However, this approach has some drawbacks. First, it relies on the hyper-parameters manually set before running the algorithm. Second, the clustering parameter T , the distance threshold between clusters, has a direct impact on both recall and precision. This requires the user has background knowledge about how to configure the clustering algorithm. Also, more clustering algorithms can be tested for better performance.

References

- [1] Kevin Hsieh, Ganesh Ananthanarayanan, Peter Bodik, Paramvir Bahl, Matthai Philipose, Phillip B Gibbons, and Onur Mutlu. Focus: Querying large video datasets with low latency and low cost. *arXiv preprint arXiv:1801.03493*, 2018.
- [2] Shaoqing Ren, Kaiming He, Ross Girshick, and Jian Sun. Faster r-cnn: towards real-time object detection with region proposal networks. *IEEE Transactions on Pattern Analysis & Machine Intelligence*, (6):1137–1149, 2017.
- [3] Ross Girshick. Fast r-cnn. In *Proceedings of the IEEE international conference on computer vision*, pages 1440–1448, 2015.
- [4] Shaoqing Ren, Kaiming He, Ross Girshick, and Jian Sun. Faster r-cnn: Towards real-time object detection with region proposal networks. In *Advances in neural information processing systems*, pages 91–99, 2015.
- [5] Kaiming He, Xiangyu Zhang, Shaoqing Ren, and Jian Sun. Deep residual learning for image recognition. In *Proceedings of the IEEE conference on computer vision and pattern recognition*, pages 770–778, 2016.
- [6] Yann LeCun, Yoshua Bengio, and Geoffrey Hinton. Deep learning. *nature*, 521(7553):436, 2015.
- [7] Alex Krizhevsky, Ilya Sutskever, and Geoffrey E Hinton. Imagenet classification with deep convolutional neural networks. In *Advances in neural information processing systems*, pages 1097–1105, 2012.
- [8] Joseph Redmon and Ali Farhadi. Yolov3: An incremental improvement. *arXiv preprint arXiv:1804.02767*, 2018.
- [9] Daniel Kang, John Emmons, Firas Abuzaid, Peter Bailis, and Matei Zaharia. Noscope: optimizing neural network queries over video at scale. *Proceedings of the VLDB Endowment*, 10(11):1586–1597, 2017.
- [10] Aaron Van den Oord, Sander Dieleman, and Benjamin Schrauwen. Deep content-based music recommendation. In *Advances in neural information processing systems*, pages 2643–2651, 2013.
- [11] Ronan Collobert and Jason Weston. A unified architecture for natural language processing: Deep neural networks with multitask learning. In *Proceedings of the 25th international conference on Machine learning*, pages 160–167. ACM, 2008.
- [12] Pierre Baldi, Peter Sadowski, and Daniel Whiteson. Searching for exotic particles in high-energy physics with deep learning. *Nature communications*, 5:4308, 2014.
- [13] Marwin HS Segler, Mike Preuss, and Mark P Waller. Planning chemical syntheses with deep neural networks and symbolic ai. *Nature*, 555(7698):604, 2018.

[14] Garrett B Goh, Nathan O Hodas, and Abhinav Vishnu. Deep learning for computational chemistry. *Journal of computational chemistry*, 38(16):1291–1307, 2017.

[15] Xiaoyu Sun, Nathaniel J Krakauer, Alexander Politowicz, Wei-Ting Chen, Qiying Li, Zuoyi Li, Xianjia Shao, Alfred Sunaryo, Mingren Shen, James Wang, et al. Assessing graph-based deep learning models for predicting flash point. *Molecular Informatics*, 39(6):1900101, 2020.

[16] Ryan Jacobs, Mingren Shen, Yuhan Liu, Wei Hao, Xiaoshan Li, Ruoyu He, Jacob RC Greaves, Donglin Wang, Zeming Xie, Zitong Huang, et al. Performance and limitations of deep learning semantic segmentation of multiple defects in transmission electron micrographs. *Cell Reports Physical Science*, 3(5):100876, 2022.

[17] Kevin G Field, Ryan Jacobs, Mingen Shen, Matthew Lynch, Priyam Patki, Christopher Field, and Dane Morgan. Development and deployment of automated machine learning detection in electron microscopy experiments. *Microscopy and Microanalysis*, 27(S1):2136–2137, 2021.

[18] Kevin G Field, Mingren Shen, Caleb P Massey, Kenneth C Littrell, and Dane D Morgan. Rapid characterization methods for accelerated innovation for nuclear fuel cladding. *Microscopy and Microanalysis*, 26(S2):868–869, 2020.

[19] Mingren Shen, Dina Sheyfer, Troy David Loefller, Subramanian KRS Sankaranarayanan, G Brian Stephenson, Maria KY Chan, and Dane Morgan. Machine learning for interpreting coherent x-ray speckle patterns. *arXiv preprint arXiv:2211.08194*, 2022.

[20] Dane Morgan, Ryan Jacobs, Mingren Shen, Priyam Patki, Matthew Lynch, and Kevin Field. Automated defect detection in electron microscopy of radiation damage in metals.

[21] Mingren Shen, Guanzhao Li, Dongxia Wu, Yudai Yaguchi, Jack C Haley, Kevin G Field, and Dane Morgan. A deep learning based automatic defect analysis framework for in-situ tem ion irradiations. *Computational Materials Science*, 197:110560, 2021.

[22] Mingren Shen, Guanzhao Li, Dongxia Wu, Yuhan Liu, Jacob RC Greaves, Wei Hao, Nathaniel J Krakauer, Leah Krudy, Jacob Perez, Varun Sreenivasan, et al. Multi defect detection and analysis of electron microscopy images with deep learning. *Computational Materials Science*, 199:110576, 2021.

[23] Nick Lawrence, Mingren Shen, Ruiqi Yin, Cloris Feng, and Dane Morgan. Exploring generative adversarial networks for image-to-image translation in stem simulation. *arXiv preprint arXiv:2010.15315*, 2020.

[24] Yilin Liu, Gregory R Kirk, Brendon M Nacewicz, Martin A Styner, Mingren Shen, Dong Nie, Nagesh Adluru, Benjamin Yeske, Peter A Ferrazzano, and Andrew L Alexander. Harmonization and targeted feature dropout for generalized segmentation: application to multi-site traumatic brain injury images. In *Domain Adaptation and Representation Transfer and Medical Image Learning with Less Labels and Imperfect Data*, pages 81–89. Springer, 2019.

[25] Sidharth Gurbani, Dane Morgan, Varun Jog, Leo Dreyfuss, Mingren Shen, Arighno Das, E Jason Abel, and Meghan G Lubner. Evaluation of radiomics and machine learning in identification of aggressive tumor features in renal cell carcinoma (rcc). *Abdominal Radiology*, 46(9):4278–4288, 2021.

[26] Adam M Awe, Michael M Vanden Heuvel, Tianyuan Yuan, Victoria R Rendell, Mingren Shen, Agrima Kampani, Shanchao Liang, Dane D Morgan, Emily R Winslow, and Meghan G Lubner. Machine learning principles applied to ct radiomics to predict mucinous pancreatic cysts. *Abdominal Radiology*, 47(1):221–231, 2022.

[27] Mingren Shen, Rui Liu, Ke Chen, and Mingcheng Yang. Diffusive-flux-driven microturbines by fore-and-aft asymmetric phoresis. *Physical Review Applied*, 12(3):034051, 2019.

[28] Shen Ming-Ren, Liu Rui, Hou Mei-Ying, Yang Ming-Cheng, and Chen Ke. Mesoscale simulation of self-diffusiophoretic microrotor. *ACTA PHYSICA SINICA*, 65(17), 2016.

[29] Mingren Shen, Fangfu Ye, Rui Liu, Ke Chen, Mingcheng Yang, and Marisol Ripoll. Chemically driven fluid transport in long microchannels. *The journal of chemical physics*, 145(12):124119, 2016.

[30] Guan-Zheng Luo, Ziyang Hao, Liangzhi Luo, Mingren Shen, Daniela Sparvoli, Yuqing Zheng, Zijie Zhang, Xiaocheng Weng, Kai Chen, Qiang Cui, et al. N6-methyldeoxyadenosine directs nucleosome positioning in tetrahymena dna. *Genome biology*, 19(1):1–12, 2018.

- [31] Nicolas Saunier Jean-Philippe Jodoin, Guillaume-Alexandre Bilodeau. Urban tracker: Multiple object tracking in urban mixed traffic. *IEEE Winter Conference on Applications of Computer Vision*, 2014.
- [32] Mengwei Xu, Mengze Zhu, Yunxin Liu, Felix Xiaozhu Lin, and Xuanzhe Liu. Deepcache: Principled cache for mobile deep vision. *arXiv preprint arXiv:1712.01670*, 2017.
- [33] Andrew B Godbehere, Akihiro Matsukawa, and Ken Goldberg. Visual tracking of human visitors under variable-lighting conditions for a responsive audio art installation. In *American Control Conference (ACC), 2012*, pages 4305–4312. IEEE, 2012.
- [34] Li Liu, Wanli Ouyang, Xiaogang Wang, Paul Fieguth, Jie Chen, Xinwang Liu, and Matti Pietikäinen. Deep learning for generic object detection: A survey. *arXiv preprint arXiv:1809.02165*, 2018.
- [35] Ross Girshick, Jeff Donahue, Trevor Darrell, and Jitendra Malik. Rich feature hierarchies for accurate object detection and semantic segmentation. In *Proceedings of the IEEE conference on computer vision and pattern recognition*, pages 580–587, 2014.
- [36] Joseph Redmon, Santosh Divvala, Ross Girshick, and Ali Farhadi. You only look once: Unified, real-time object detection. In *Proceedings of the IEEE conference on computer vision and pattern recognition*, pages 779–788, 2016.
- [37] Liadan O’callaghan, Nina Mishra, Adam Meyerson, Sudipto Guha, and Rajeev Motwani. Streaming-data algorithms for high-quality clustering. In *Data Engineering, 2002. Proceedings. 18th International Conference on*, pages 685–694. IEEE, 2002.
- [38] Feng Cao, Martin Estert, Weining Qian, and Aoying Zhou. Density-based clustering over an evolving data stream with noise. In *Proceedings of the 2006 SIAM international conference on data mining*, pages 328–339. SIAM, 2006.

7 Appendix

7.1 Training Curves

The models converge after about 50 to 100 learning epochs and the accuracy of evaluation comes to or above 95%. The learning curves for ResNet-50, ResNet-152

and the remaining part of ResNet-152 after two cuts is shown in Figure 4, Figure 5, Figure 6, Figure 7.

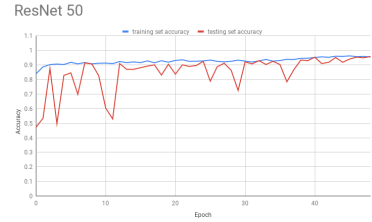


Figure 4: Training Curves of ResNet-50

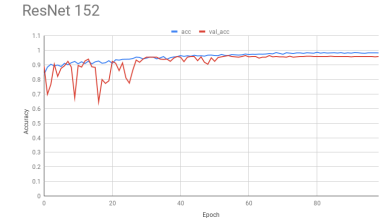


Figure 5: Training Curves of ResNet-152

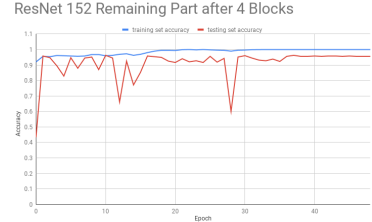


Figure 6: Training Curves of ResNet-152 cutting 4 blocks

7.2 Source Code of this Project

We provide all the source code of this project on Github and you check the code from this link, https://github.com/iphyer/FocusIngestOpt_FinalProject_CS744Fall2018.

The code is built on Python3 and Keras with Tensorflow as back-end engine.

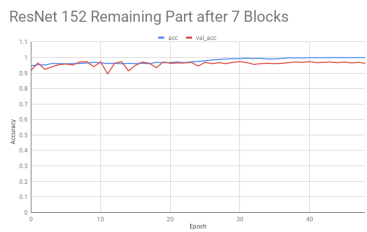


Figure 7: Training Curves of ResNet-152 cutting 7 blocks